Atmospheric Pressure Plasma Based Fabrication of Paper Biosensors

Dr Ram Prasad Gandhiraman
Universities Space Research Association
NASA Ames Research Center
Moffett Field, CA
ramprasad.gandhiraman@nasa.gov

Research Area

In-situ Resource Utilization for Mars Mission

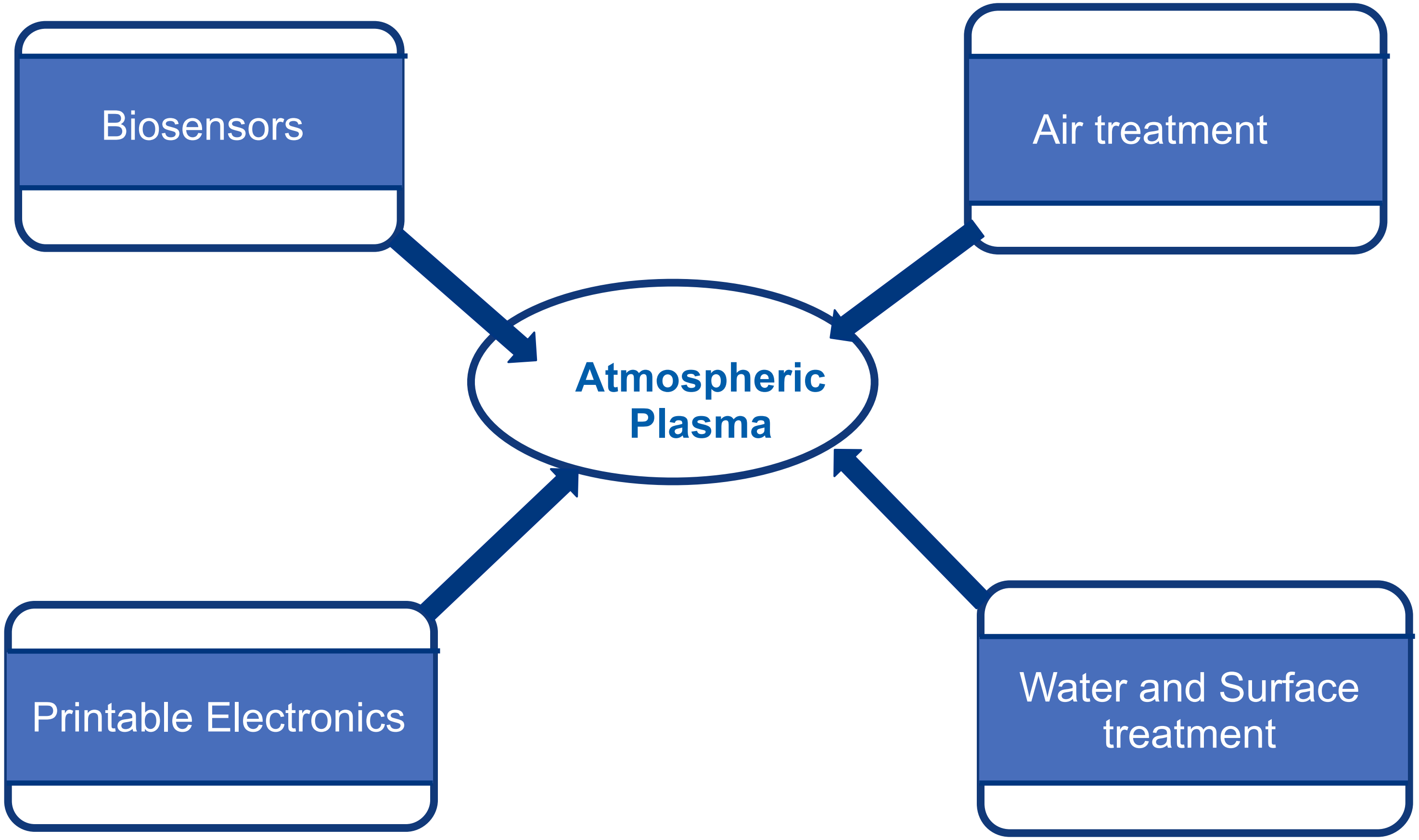

Funding
NASA Advanced Exploratory Systems (AES)
NASA ARC Center/Director's Innovation Fund
NASA Innovative Advanced Concepts (NIAC)

Technologies for Space Mission

Image source: Nasa Ames

- NASA’s manned mission to Mars in 2030’s
- NASA’s Orion Multi-purpose Crew Vehicle - human missions beyond LEO
- Public and Private Outer Space Explorations
- Currently 1 year long mission in ISS by NASA astronauts and Russian cosmonauts
- Mars 500 mission by Russia, China and ESA-finished in 2011. 520 days of isolation to study the effect of isolation on human physiology and psychology.
- NOT enough data on changes in human physiological conditions in space
- **Insitu resource utilization -Mars mission**

Biosensors

A Biomarker is a parameter that can be used to measure the presence of or severity or progress of some disease or the effects of treatment. The parameter can be chemical, physical or biological.

- sample
- Fluidic channel
- antibody engineering
- recognition and capture ↔ Surface Functionalisation
- Signal Transduction ↔ Nanomaterials

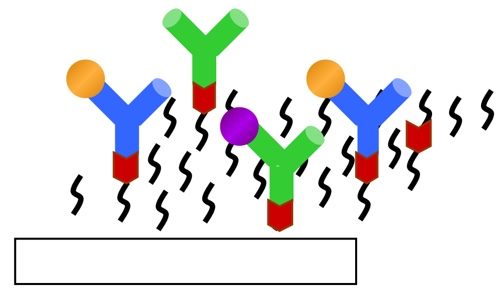

Key scientific and technological goals

- Reliable and reproducible fabrication of paper sensors
- Efficient surface functionalisation for flow control, biomolecule attachment and reduced non-specific binding
- Incorporation of nanostructures for signal transduction/ amplification(Gold NPs, CNT)
- DNA hybridization

Surface Functionalization

- To retain biologiocal activity of the ligand
- Physisorption
    - ❖ Protein conformational change
    - ❖ Loss of antigen binding activity
- To minimise non specific binding - High signal to noise
- Film wettability, surface roughness
- To achieve high immobilization yield
- To ensure reproducibility and reliability of measurement
    - NH2- Amines; COOH – Carboxy;
    - SH – Mercapto; $(OH)_n$ poly ethylene glycol (PEG)

Paper Based Biosensors

Why Paper Sensors:

- Healthcare technologies for long duration mission require: low weight & long shelf life or easy fabrication,
- Cellulose: Light weight, capillary flow – independent of gravity, in-space fabrication
- Bacterial cellulose can be prepared using synthetic biology in Mars

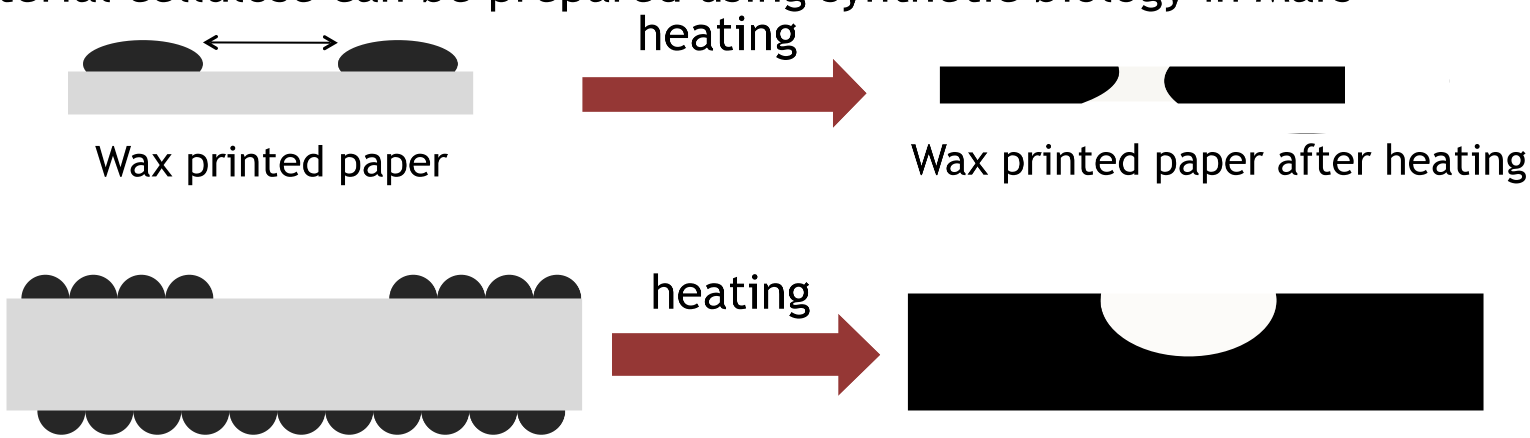

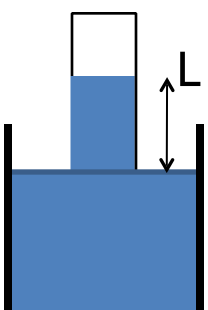

surface tension

pore diameter

distance

$$L = \sqrt{\frac{\gamma D t}{4\eta}}$$

time

viscosity

Washburn equation

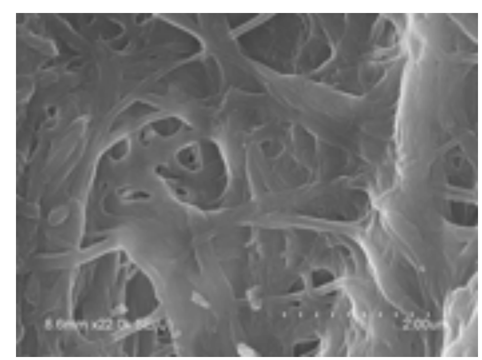

Fabrication of Biosensor Chips

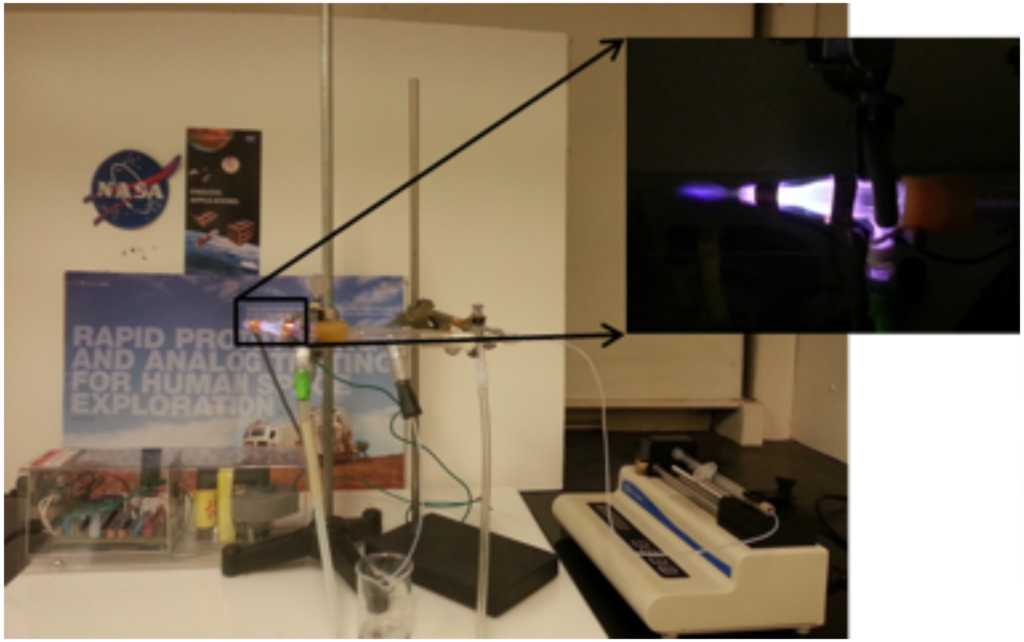

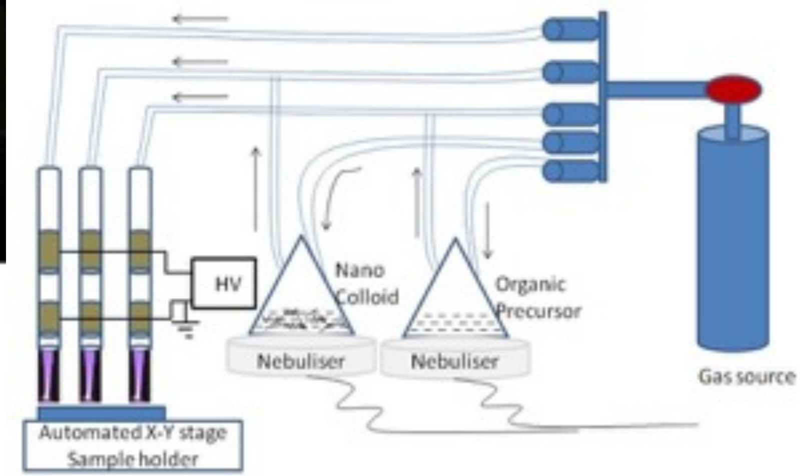

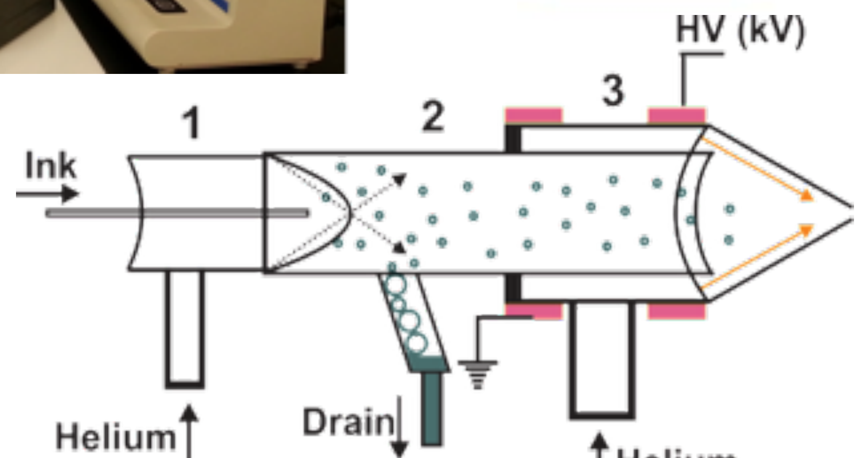

- Can form fluidic channels, patterning, organic functionalities, nanostructures in pape
- Gandhiraman et al., US Patent application 14/515, 072

Fabrication of Biosensor Chips

Organic functionalization & nanomaterial deposition

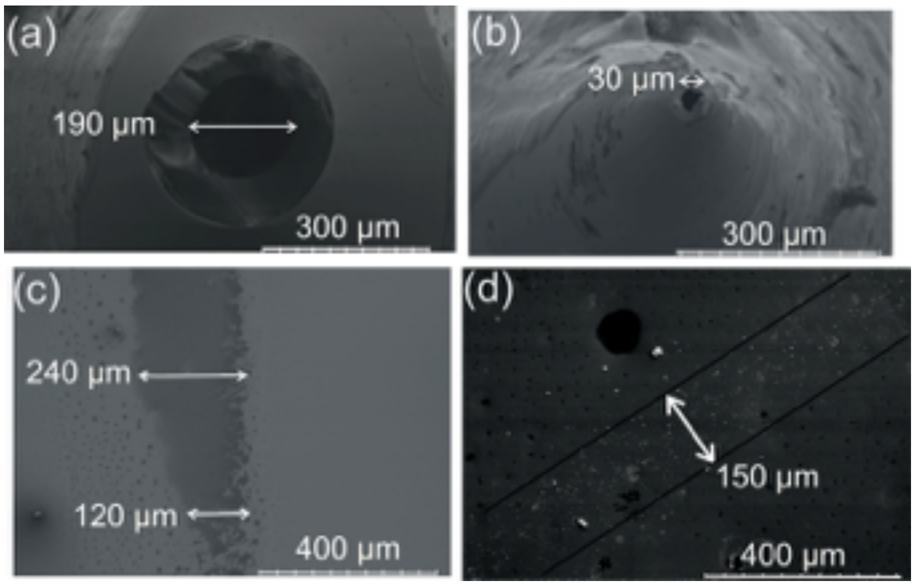

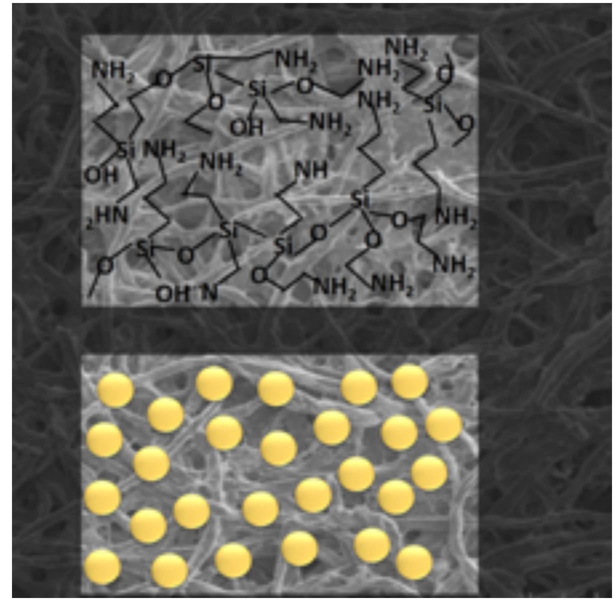

Wax coated paper

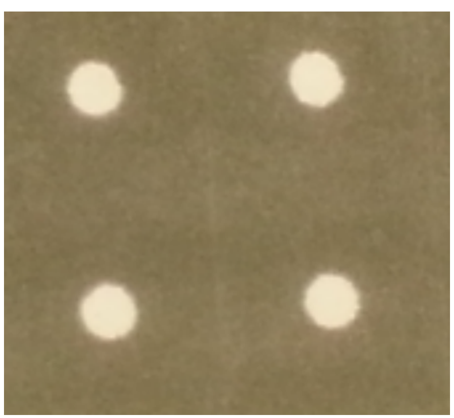

Plasma functionalized paper

SEM

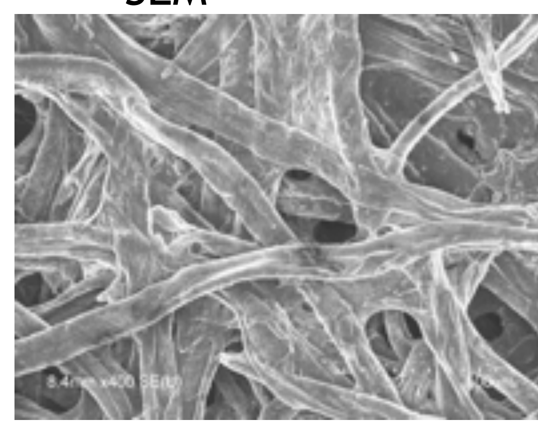

DNA Hybridization

Amine functionalization for covalent binding
Polyethylene glycol (PEG) functionalization for reduced non-specific binding

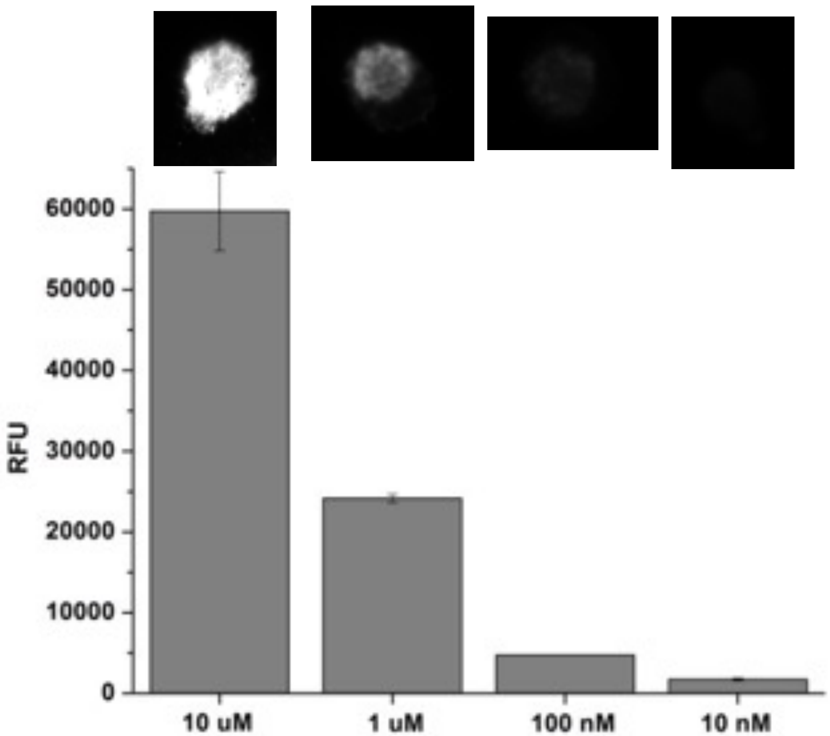

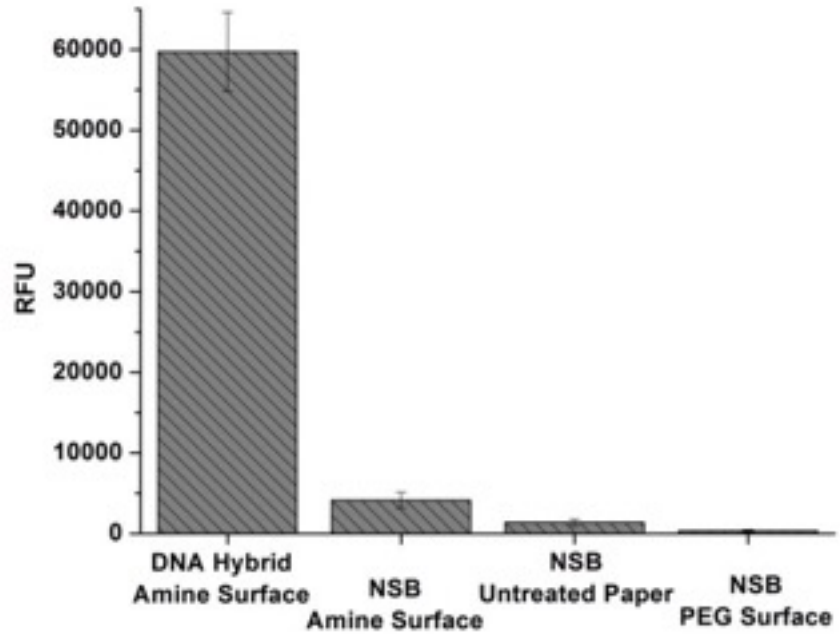

Gandhiraman et al., ACS Applied Materials & Interfaces 2014, 6, 22751

Nanomaterials Deposition

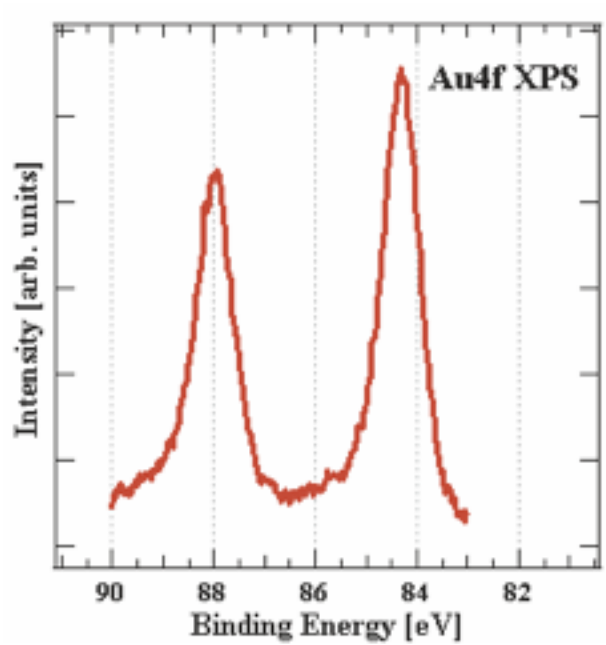

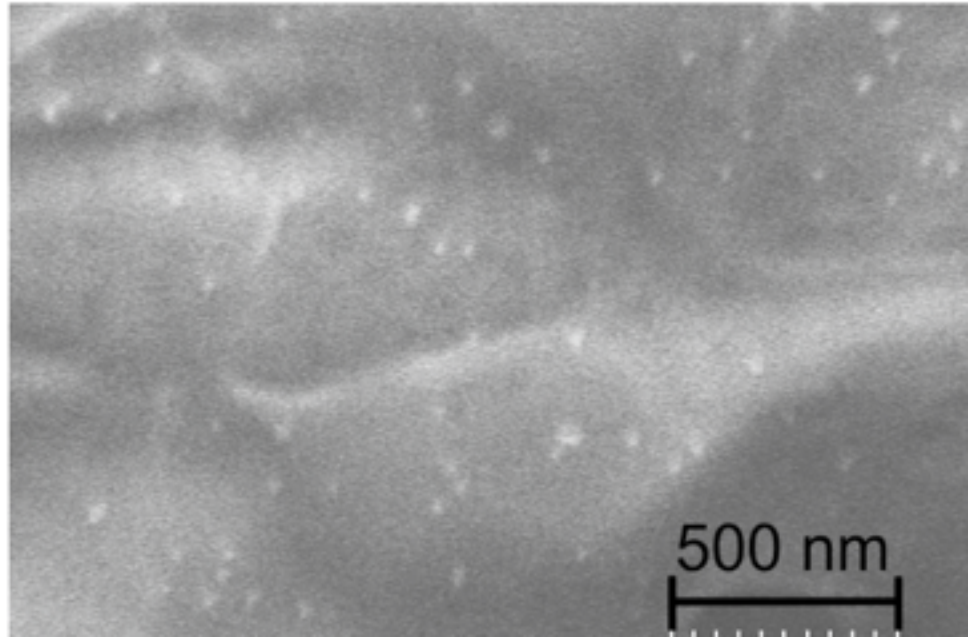

Cellulose

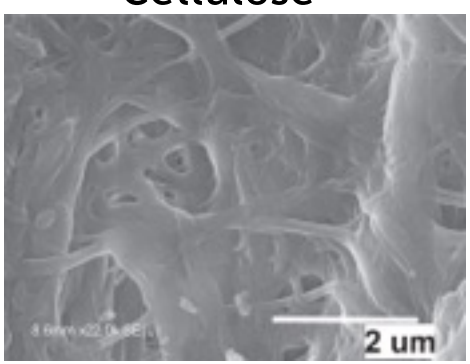

Silver nanowire

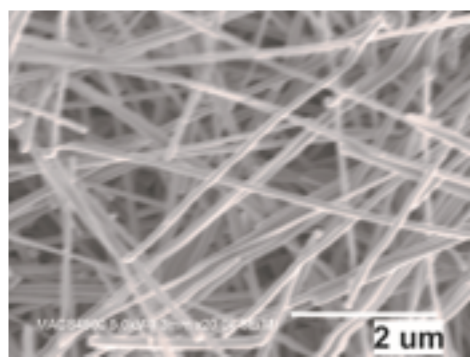

Silver nanowire coated cellulose

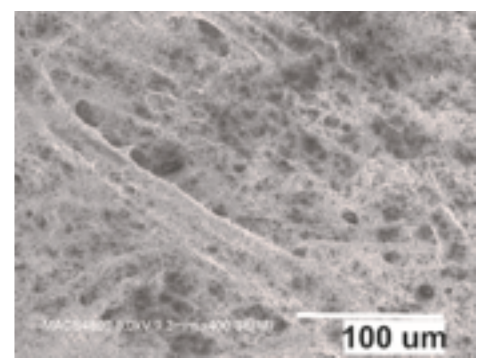

Functionalization & Signal Amplification

Aminated DNA containing Cy3 Fluorophore

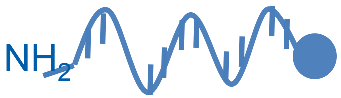

NH_2 ssDNA on Gold –Strong binding

NH_2 ssDNA on aminated (Aptes) surface – repulsion

NH_2 ssDNA on PEG surface - repulsion

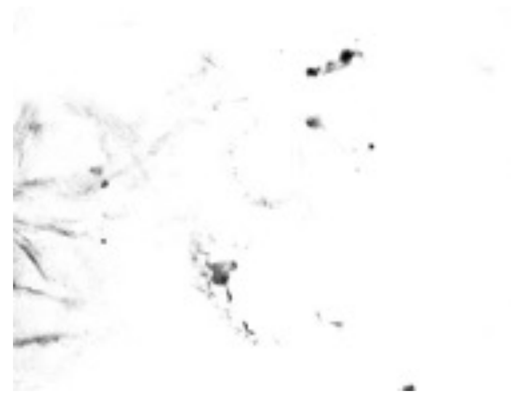

Gold nano particle (NP)

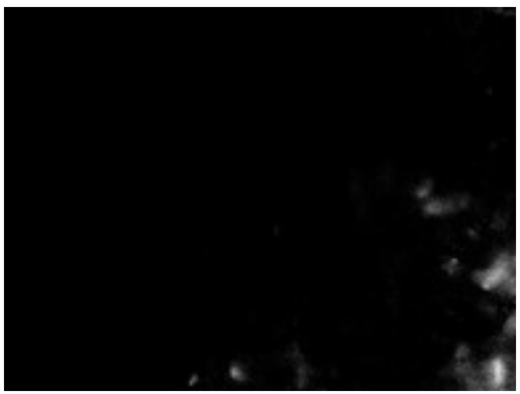

Amine Surface

Amine + Gold NP

PEG Surface

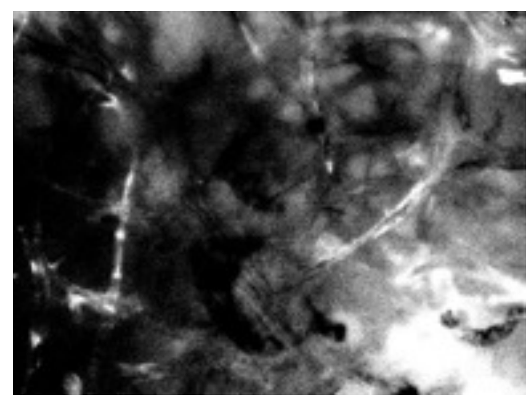

PEG + Gold NP

Infrared Spectroscopy

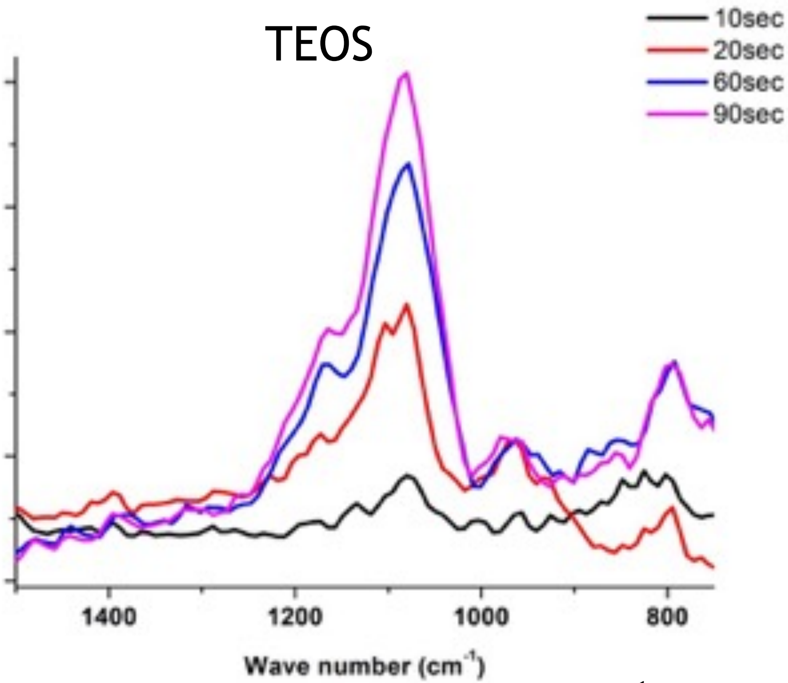

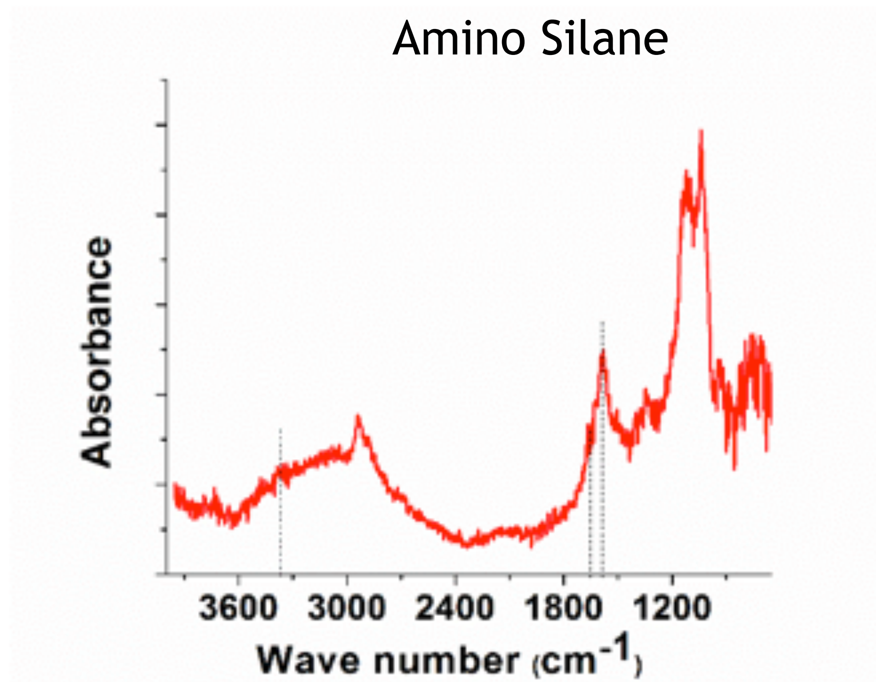

Multiple bands between 2800 and 3000 cm^{-1} C–H vibrations in the ethyl components

Intense bands between 800 and 1200 cm^{-1} arise from Si–O molecular vibrations of the ortho silicate component of the precursor.

Asymmetric and symmetric N–H stretching bands between 3380 - 3350 cm^{-1} and between 3310 - 3280 cm^{-1}

N–H deformation between 1650 cm^{-1} and 1580 cm^{-1}

N–H bending vibration of free amine 1630 cm^{-1}

N–H bending vibration of amine group, which is hydrogen-bonded either to hydroxyl groups in silanol in the bulk of the film or to cellulose at the interface 1585 cm^{-1}

X ray Spectroscopy

X ray photons with energy level close to the core level excitation is incident on the sample, transition of the core level electrons to unoccupied valence orbitals takes place upon absorption of photon energy.

C 1s XPS

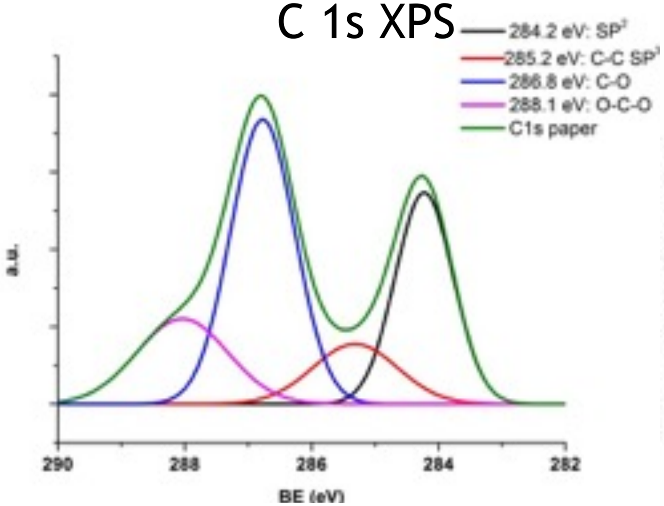

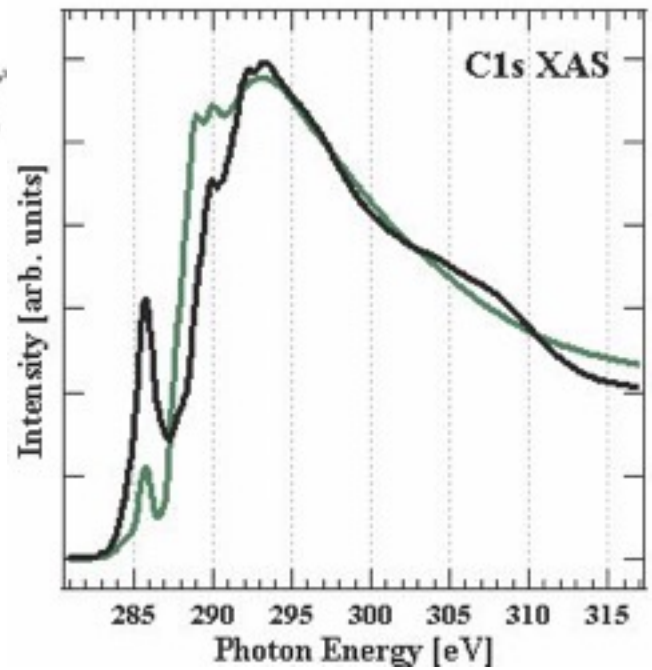

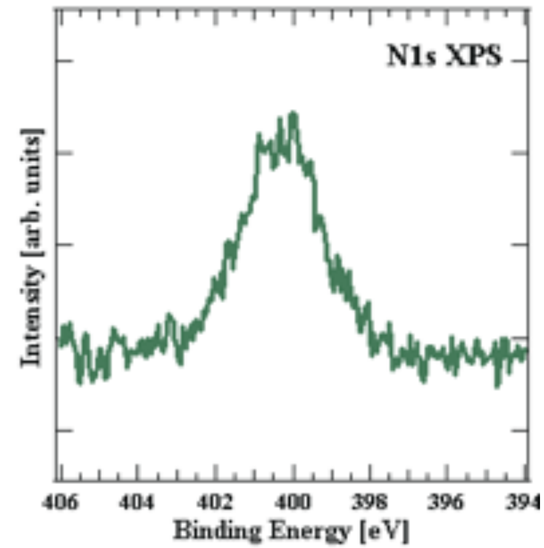

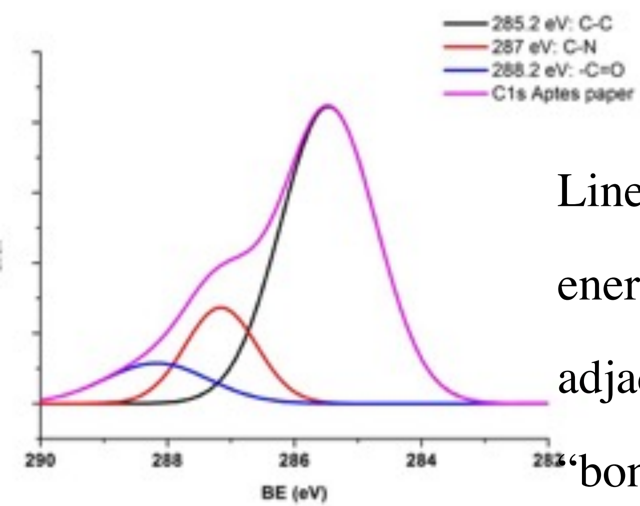

Linear relationship between σ* transition energies and bond lengths to atoms adjacent to the core excited atom, “bond-length with a ruler

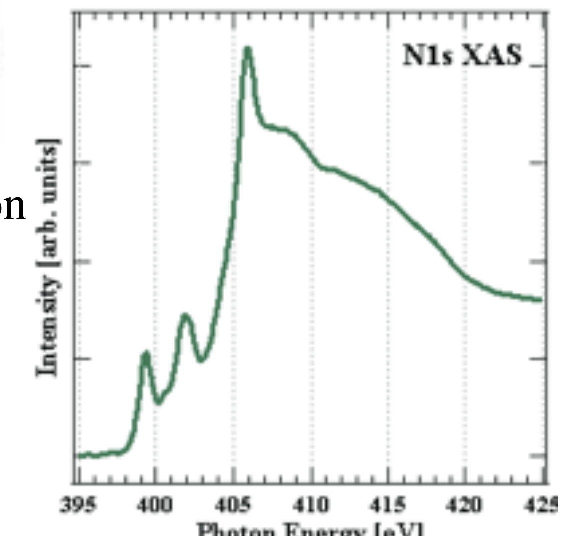

Table 1. C K-Edge NEXAFS Peak Positions and Attribution

cellulose	aminated cellulose	assignments
284.8 eV (shoulder)	284.8 eV (shoulder)	probably beam damage
		π^* C=C
285.9 eV (intense)		π^* C≡C
		(σ^* at 308)
	286 eV (intense)	π^* C=N
	287.8 eV shoulder	carbonyl C=O π^*
288.1 eV (shoulder)		probably corresponds to excitations into orbitals of dominantly C−H* resonance
	289.1 eV (intense)	σ^* CNH
	clearly not present in cellulose	σ^* CH and 1s−3p Rydberg (Rydberg mixed-valence transitions)
290.1 eV (intense)	290.2 eV (intense)	1s to σ^* C−H/3p
		σ^* C−H
292.5 eV intense	292.5 eV broad	C−H resonance
		alkanes, C−C σ^*
293.5 eV (intense)	293.4 eV (intense broad)	C−O σ^*
297 eV (broad)		σ^* O−C−O
	299 eV (broad)	1s to σ^* C−N of carbon in −CONH
304 eV broad		σ^* C=C
309 eV (broad)		σ^* C≡C
	308 eV	C=O σ^*

Table 2. N K-Edge NEXAFS Peak Positions and Attribution

peak position	assignment
399.3 eV (intense)	π^* N=C
400.6 eV (minor)	π^* C≡N/σ^* N−H
401.9 eV (intense)	π^* CONH
404.8 eV (shoulder)	nitro compound
405.9 eV (intense)	σ^* N−C
	σ^* NH2
408.9 eV (shoulder)	σ^* NH
411 eV broad	σ^* N=C
	σ^* CONH

Plasma Surface Functionalisation

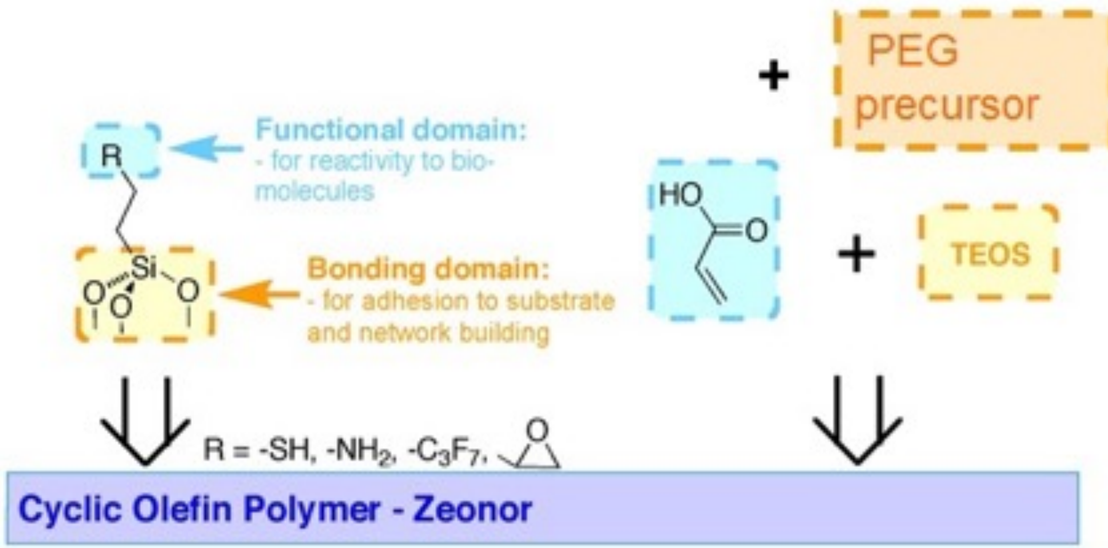

Carboxy Functionalisation on Plastic

Sequential deposition of Tetra ethyl ortho silicate and Acylic acid

Teos: Adhesion and network building layer
Acrylic acid: carboxy functionality

Percentage Carboxy :
6.5% in Acrylic acid
16.4% in Teos AA coating

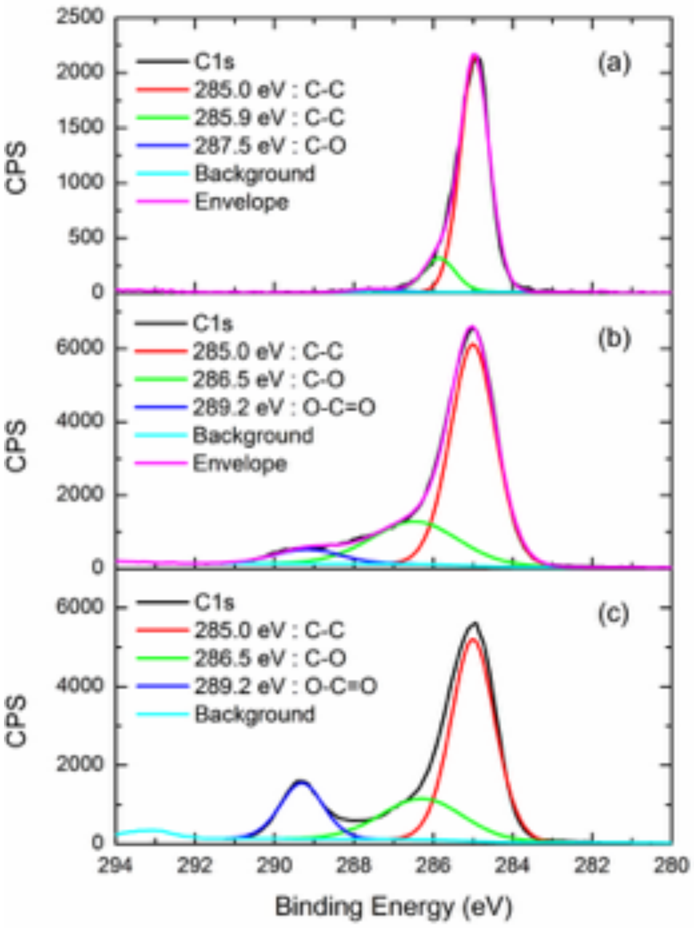

Zeonor

Acrylic

Teos
+
Acrylic

Plasma Functionalisation on Gold

Carboxy functionalities are deposited on gold surface by plasma enhanced chemical vapor deposition (PECVD)

1) Siloxane as an adhesion layer on gold using Tetra ethyl orthosilicate (Teos)
   Sequential deposition of acrylic acid for carboxy functionalisation

2) Mercapto silane deposition- Mercapto group adhesion layer on gold, siloxane for network building for further functionalisation
   Sequential deposition of acrylic acid for carboxy functionalision

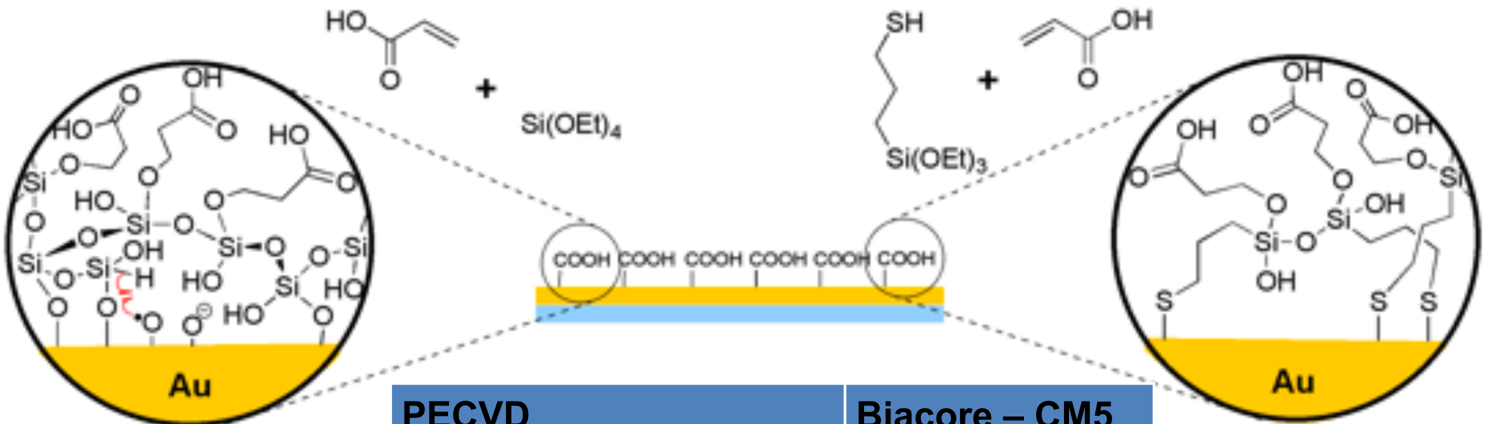

PECVD	Biacore – CM5
<10 mins	12 hrs to 24 hrs
No refrigeration required Reduced cost due to bulk production	storage in fridge Sq.cm chip costs 120 euro.

Infrared Red Spectroscopy and SIMS

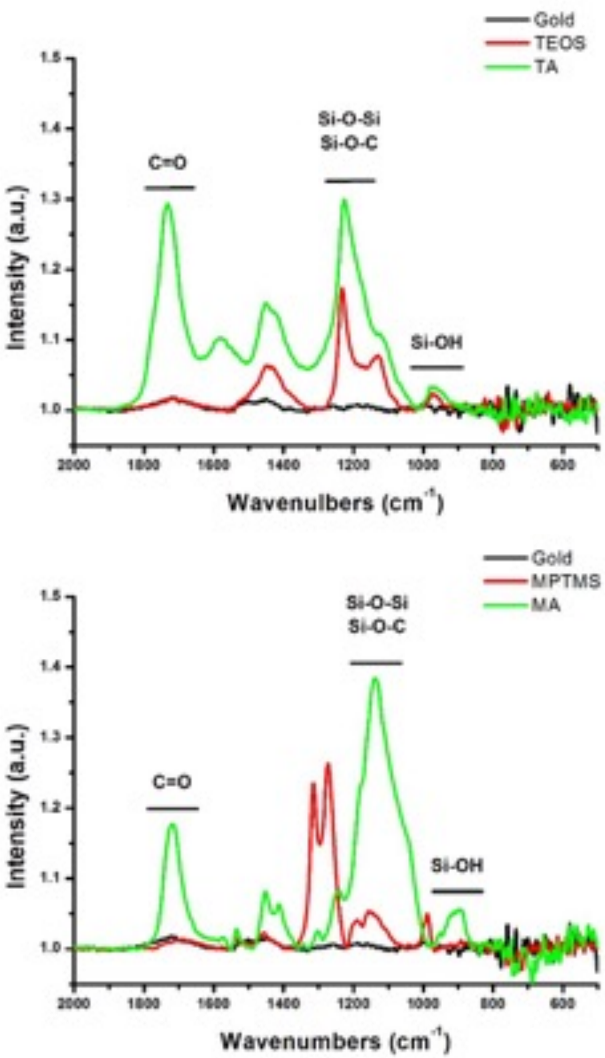

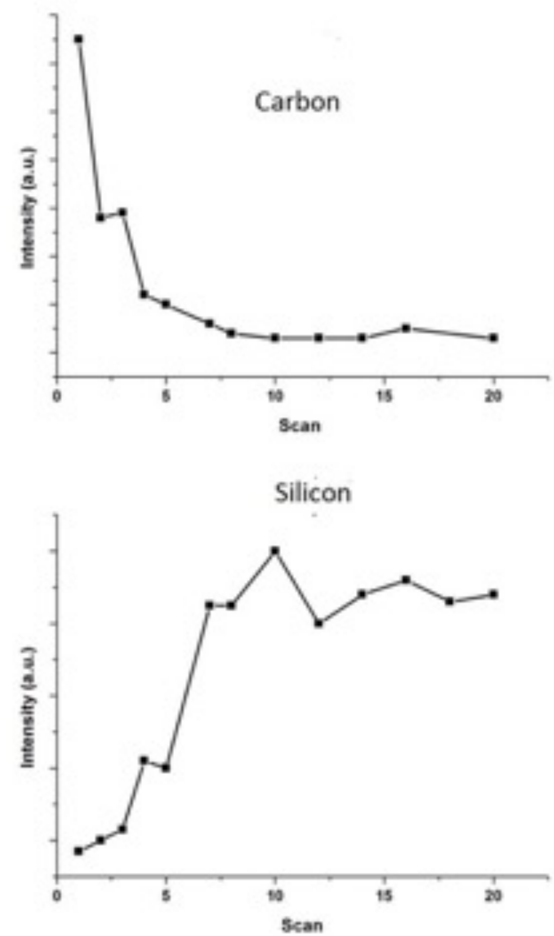

XPS – Quantitative analysis

Sample	C-C	C-S	C-O	O-C=O
Binding energy (eV) % Area of Peak				
TA	285.0 60.8%		286.5 20.2%	289.1 19.0%
MA		285.4 39.0%	286.5 8.9%	289.0 2.1%

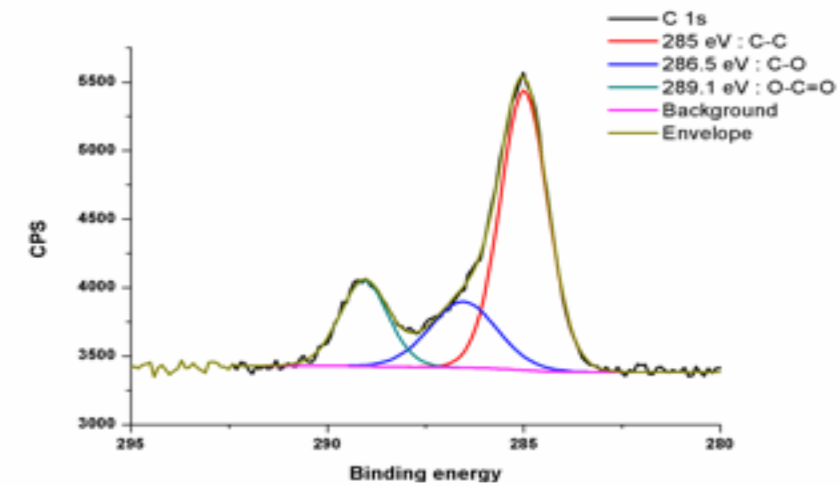

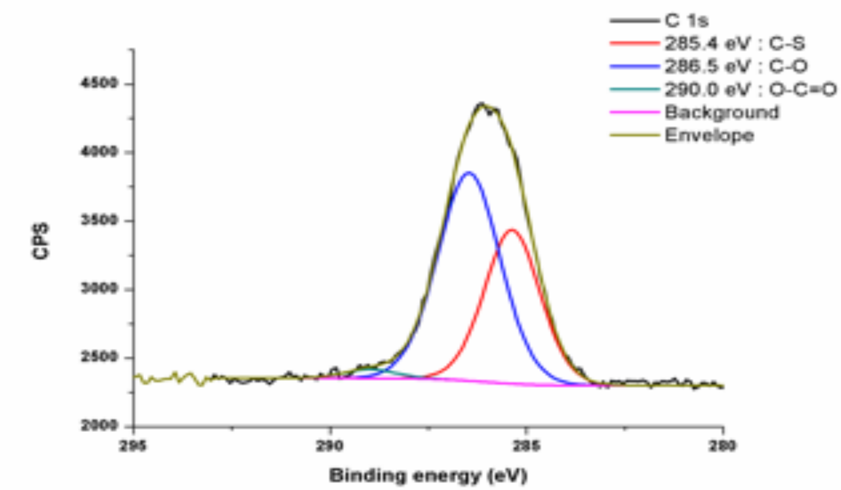

Percentage carboxy group has increased from 2.1% in mercapto based coating to 19.1% in Teos/AA coating

DNA Attachment Studies

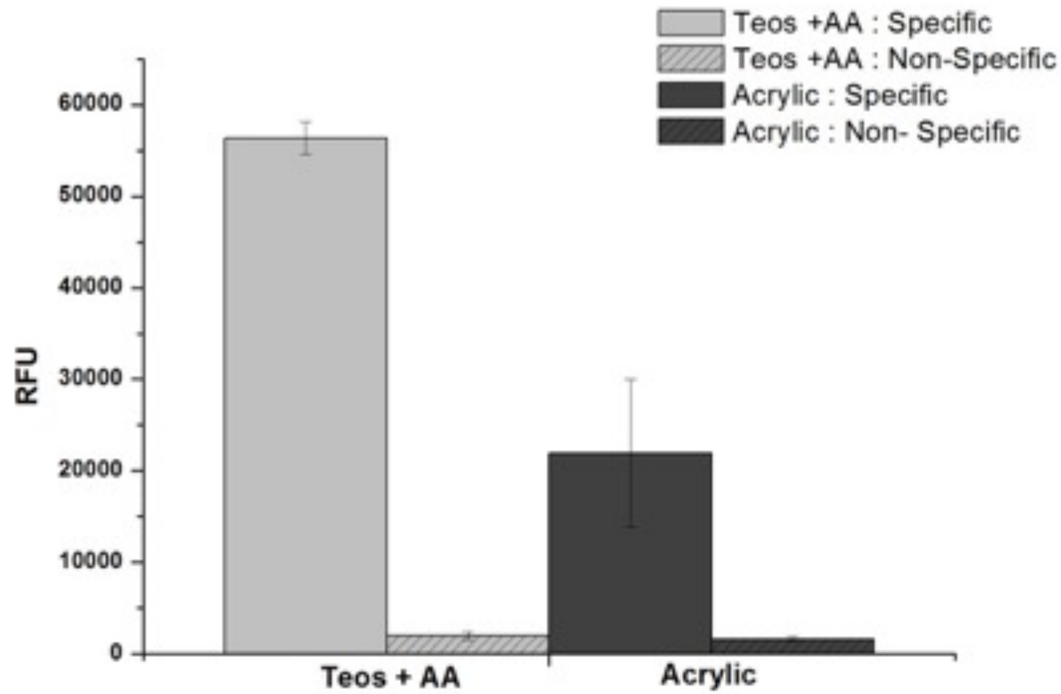

Specific binding: attachment of Cy-5 labelled amino terminated DNA
Non specific binding: attachment of Cy-5 labelled DNA without NH2

Samples Treated with Whole Blood

SiOCH

COOH

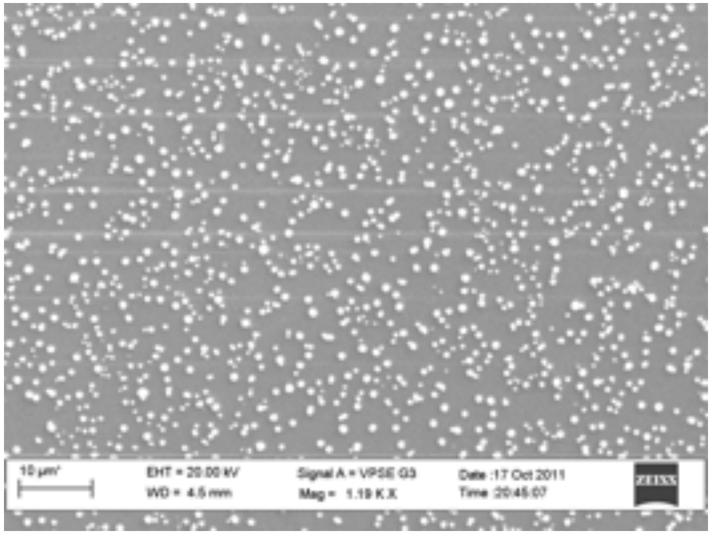

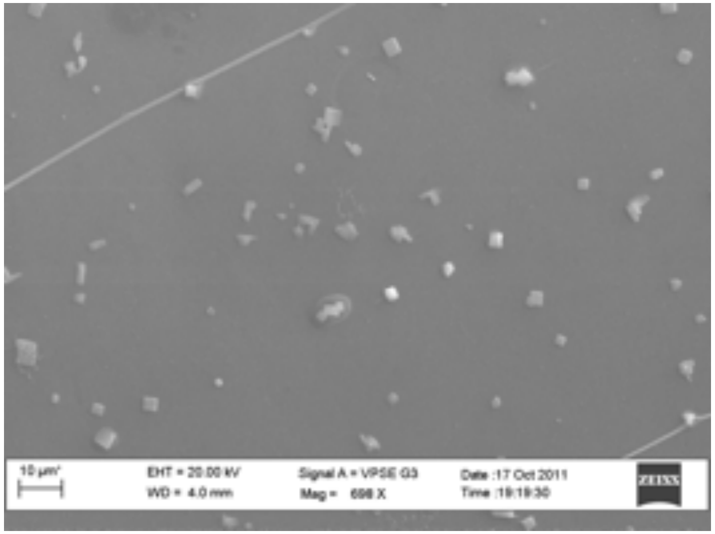

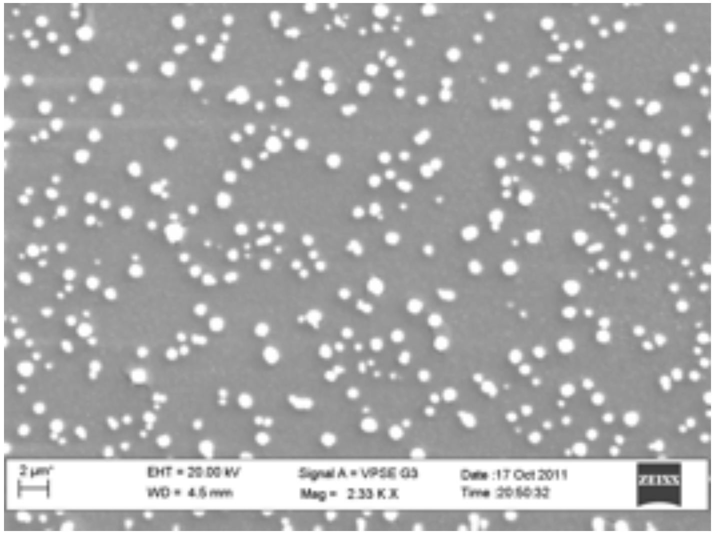

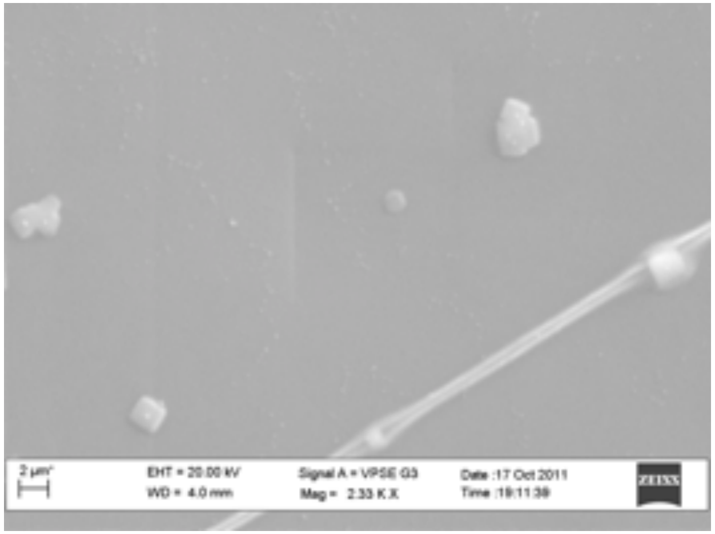

Whole Blood - Labelled Detection of NSB

SiOCH coating

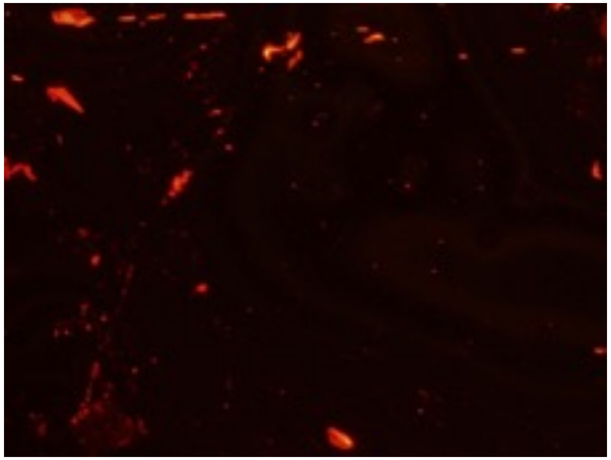

Fibrinogen capture layer

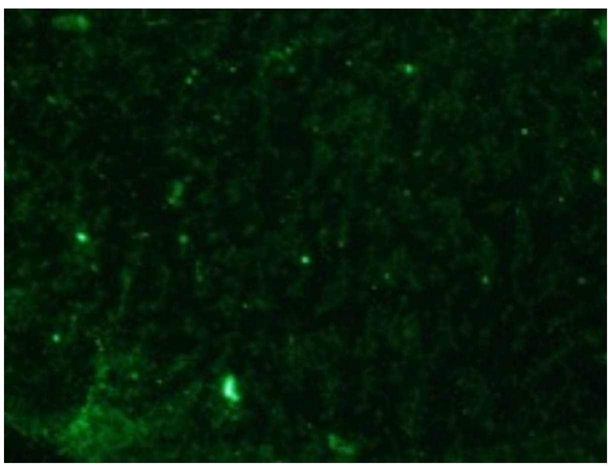

Platelets bound from whole blood

Carboxy coating

Fibrinogen capture layer

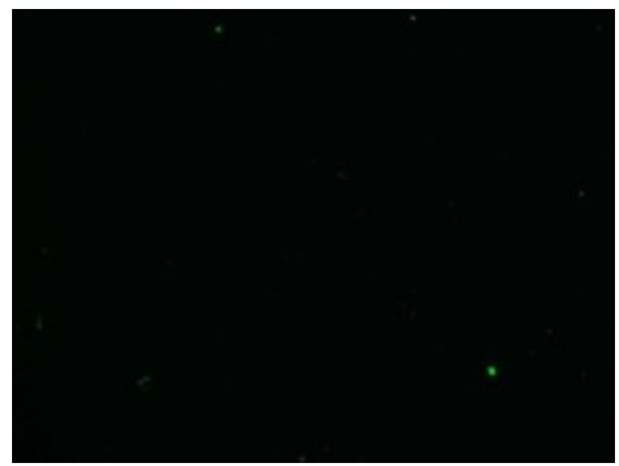

Platelets bound from whole blood

Commercial Chips

http://www.gelifesciences.com

PURCHASE ORDER

CM5 chips - DCU
GE Healthcare UK Ltd
Amersham Place
Little Chalfont
Buckinghamshire
HP 7 9NA
UK
United Kingdom

Order Number	**300136795**
Order Date	12/04/2011
Supplier Number	10091
Requisitioned By	Ram Gandhiraman
Authorised By	Mary Fallon

Tax Clearance: Q072611 Certificate Expiry Date: 13/10/2011

Deliver To:

BDI
Dublin City University
Collins Avenue
Dublin 9
Ireland

Invoice To:

Dublin City University
Finance office
Dublin City University
Glasnevin
Dublin 9

Dr. Ram Prasad Gandhiraman

	PRODUCT CODE	DESCRIPTION	QTY	UNIT	UNIT PRICE	VAT %	NET AMOUNT (EX VAT)	GROSS (INC VAT)
1	40000	Br-1000-12 CM5 sensor chips	1.0	EA	410.00	0.0	410.00	410.00
2	40000	BR-1000-50	1.0	EA	263.00	0.0	263.00	263.00
3	40000	Shipping charge	1.0	EA	30.00	0.0	30.00	30.00

http://www.gelifesciences.com

Cell-Based Assays, Immunoassays, Biochemical Assays, Accessories, and Reagents
Electrophoresis, Blotting & Detection
Label-Free Analysis Technologies
Microcalorimetry
Surface Plasmon Resonance (SPR)
Accessories
Food Analysis
Reagents, Buffers, Solutions
Sensor Chip
Sensor Chip Au
Sensor Chip C1
Sensor Chip CM3

Overview | Product Data | Related Documents | Product Support

Sensor Chip CM5, pack of 3

The most versatile chip available – the first choice for immobilization via -NH2, -SH, -CHO, -OH or -COOH groups.

- Use for immobilization via $-NH_2$, -SH, -CHO, -OH, or -COOH groups.
- Suitable for ligand fishing.
- Suitable for high capacity capture.
- Supports a wide range of immobilization levels.
- Attach proteins, nucleic acids, carbohydrates or small molecules.

Matrix: carboxymethylated dextran covalently attached to a gold surface. Molecules are covalently coupled to the sensor surface via amine, thiol, aldehyde or carboxyl groups. Interactions involving small organic molecules, such as drug candidates, through to large molecular assemblies or whole viruses can be studied. A high binding capacity gives a high response, advantageous for capture assays and for interactions involving small molecules. High surface stability provides accuracy and precision and allows repeated analysis on the same surface.

Product Catalog
Analytical Technologies
Automated Sequencing
Cell Analysis and Imaging
Cell-Based Assays, Immunoassays, Biochemical Assays, Accessories, and Reagents
Electrophoresis, Blotting & Detection
Label-Free Analysis Technologies
Microcalorimetry
Surface Plasmon Resonance (SPR)
Accessories
Food Analysis
Reagents, Buffers, Solutions
Sensor Chip
Sensor Chip Au

Product Name: Sensor Chip CM5, pack of 3

Price: On request

Quote

Product code: BR100012

Overview | Product Data | Related Documents | Product Support

Sensor Chip CM5, pack of 3

Complete Packsize	3 pieces
Application	For most interaction analyses in Biacore systems.
Includes	3 x sensor chips
Surface	Carboxymethylated dextran covalently attached to a gold surface.
For Use With	Biacore X100, Biacore 3000, Biacore 2000, Biacore 1000, Biacore Upgrade, Biacore X, Biacore C, and Biacore J
Storage Conditions	11 REFRIGERATED
Min. Order Quantity	1

Comparision with Biacore/GE Lifesciences

Samples	Response Units (anti-IgG)	Mass density (ng/mm²)	Response Units (IgG)	Mass density (ng/mm²)	Fibrinogen	Mass density of Non specifically bound Fibrinogen (ng/
PECVD	3874.0	3.9	588 (15ng/mL)	0.6	1 mg/mL	0.14
CM5 dextran (GE Life sciences)	7149.0	7.2	810 (15 ng/mL)	0.8	1 mg/mL	0.06

	PECVD	Biacore - CM5
Deposition time	*<10 mins*	*12 hrs to 24 hrs*
Cost	*High initial investment, low running cost, Several hundred chips can be deposited in an hour*	*No initial investment, high manual intervention, Each chip costs 135 euro.*
Sensitivity	*Performs similar to Biacore chips*	*Highly sensitive*
Stability	*Highly stable over long period of time - No refridgeration necessary*	*Long chain films poor stability- storage in fridge*
Organic wastes	*None*	*Industrial liquid wastes*

Gandhiraman et.al., ACS Applied Materials and Interfaces 2011, *3* (12), pp 4640–4648

Surface Plasmon Enhanced Ellipsometry

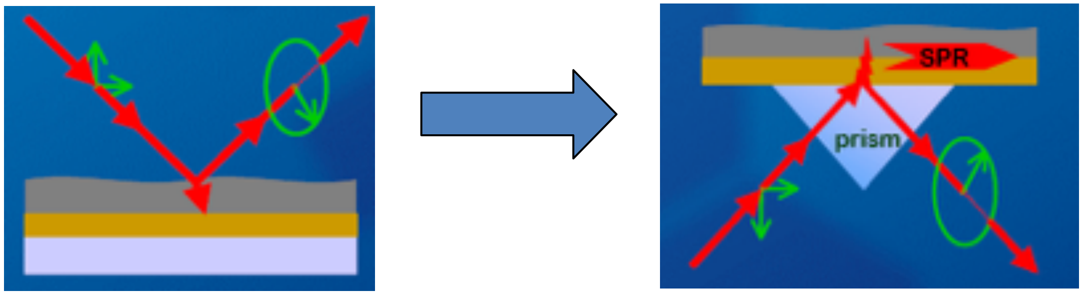

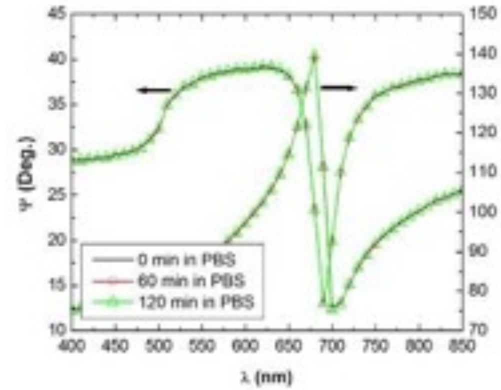

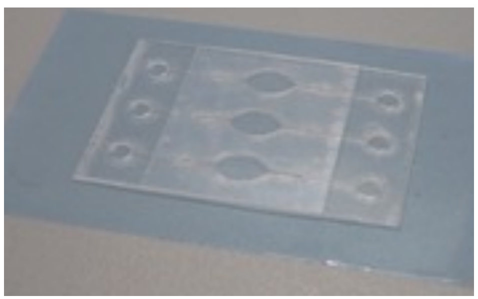

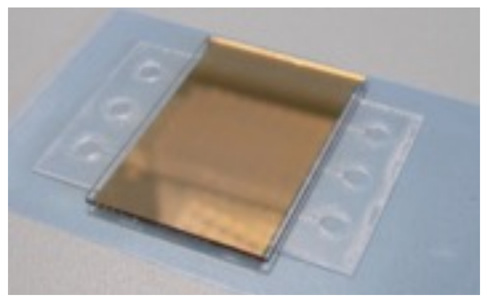

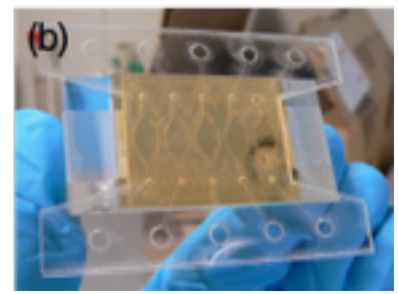

Poksinski, M. [2003],
Total Internal Reflection
Ellipsometry,
1st ed, Institute of
Technology,
Linköping University.
Licentiate Thesis No. 1016

Ellipsometry

- Linearly polarized light upon reflection becomes elliptically polarized.
- Fresnel reflection co-efficients of p and s components are different
- phase change of the reflected field relative to the incident field occurs, depending on the refractive indices of the materials involved

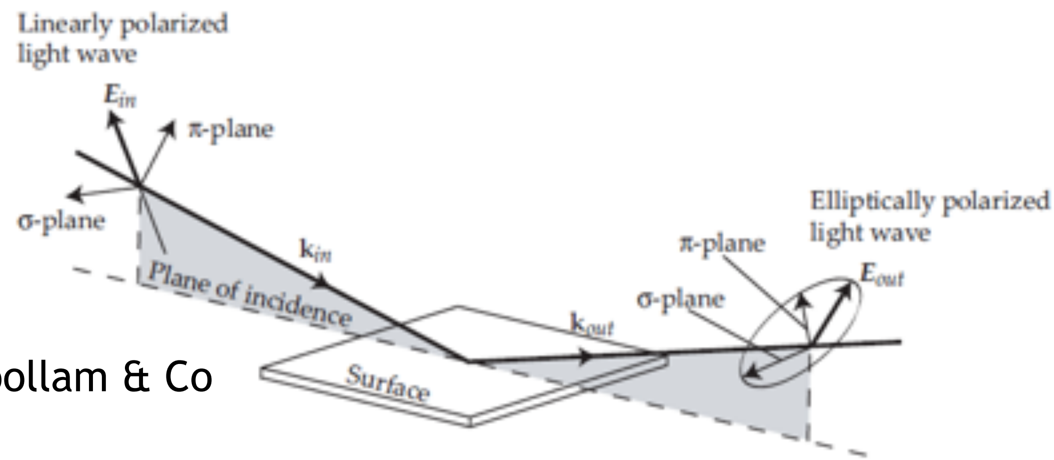

J.A. Woollam & Co

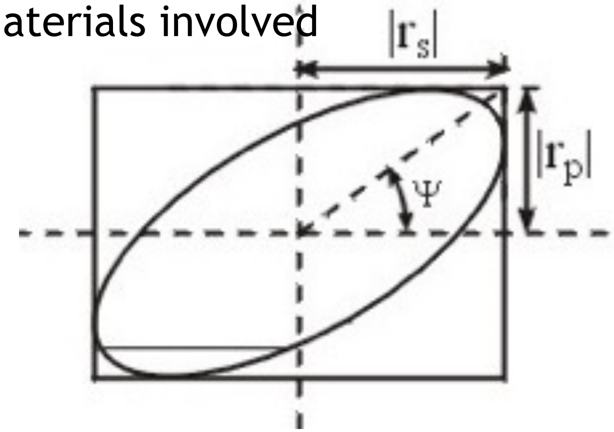

Relative attenuation of s and p polarized light determines tilt of ellipse **(psi) ψ**

Relative phase shift of s and p polarized light is related to ellicicity of ellipse **(delta) Δ**

- r_s, r_p: normalized amplitude of *s* and *p* component after reflection;
- tan(Ψ): amplitude ratio upon reflection and Δ: phase shift

$$\tan\Psi = \frac{|R^p|}{|R^s|}$$

$$r_{12}^{p} = \frac{\tilde N_2\cos\phi_1 - \tilde N_1\cos\phi_2}{\tilde N_2\cos\phi_1 + \tilde N_1\cos\phi_2} \qquad r_{12}^{s} = \frac{\tilde N_1\cos\phi_1 - \tilde N_2\cos\phi_2}{\tilde N_1\cos\phi_1 + \tilde N_2\cos\phi_2}$$

$$R^{p} = \frac{r_{12}^{p} + r_{23}^{p}\exp(-j2\beta)}{1 + r_{12}^{p}r_{23}^{p}\exp(-j2\beta)} \qquad R^{s} = \frac{r_{12}^{s} + r_{23}^{s}\exp(-j2\beta)}{1 + r_{12}^{s}r_{23}^{s}\exp(-j2\beta)}$$

$$\rho = \frac{R^p}{R^s} \qquad \rho = \tan\Psi\, e^{j\Delta}$$

Surface Plasmon Resonance

Surface plasmons- collective electron density waves propagating at the interface between metal and dielectric

<u>Metal- dielectric interface</u>

At certain launch angle resonance occurs, when the wave vector of the component of the incident light parallel to the metal surface is equal to the wave-vector of the surface plasmons. A travelling wave parallel to the surface alone exists while the amplitude of the electric field exponentially decays along the surface perpendicular direction. Energy of the incident photon is then absorbed by surface charge density.

The wave vector of the surface plasmon oscillations K_x is defined as,

$$K_x = \frac{2\pi}{\lambda}\left(n_m^2 \times n_d^2 \Big/ n_m^2 + n_d^2 \right)$$

n_m = refractive index of the metal ; n_e= refractive index of the dielectric material.

The refractive index of the silver films is higher than that of gold, they exhibit longer and enhanced evanescent field and hence more sensitive than gold

Surface Plasmon Resonance

An electromagnetic plane wave that propagates in a medium with refractive index n can mathematically be described by an electric field E:

$$E = E_0 \exp(j\omega t - j\mathbf{k}\cdot\mathbf{r}) = E_0 \exp\left(j\omega t - jk_x x - jk_y y - jk_z z\right)$$

wavevector **k**: its direction is parallel to that of the wave propagation; its magnitude is

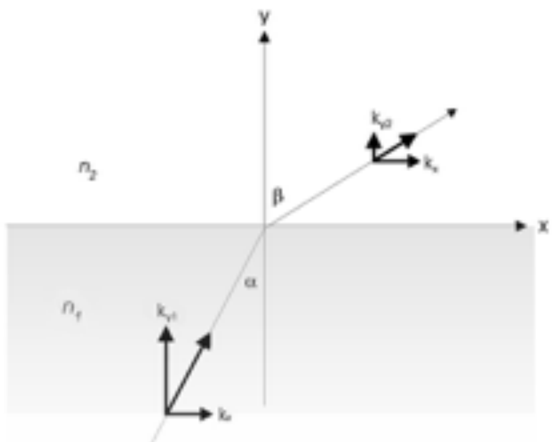

$$k = \sqrt{k_x^2 + k_y^2 + k_z^2} = n\frac{2\pi}{\lambda} = n\frac{\omega}{c}$$

$$n_1 \sin\alpha = n_2 \sin\beta \qquad\qquad k_{x_1} = k_{x_2} \equiv k_x$$

$$k_{y_2}^2 = n_1^2\left(\frac{2\pi}{\lambda}\right)^2\left(\frac{n_2^2}{n_1^2} - \sin^2\alpha\right)$$

For $\sin\alpha > n_2/n_1$ right part is negative and Ky is imaginary

$$E_2 = E_0 e^{-\kappa_{y2} y}\exp(j\omega t - jk_x x)$$

In medium 2 there is only a travelling wave parallel to the interface, with the amplitude of the electric field exponentially decaying along the y direction

Maximising SPR Sensing

Effect of thickness of the metal layer

To obtain maximum SPR sensitivity, it is advantageous to have the reflected light intensity as minimum as possible at the SPR wavelength.

If the metallic film is too thick that the evanescent wave decays before reaching the dielectric area. T he evanescent wave decays within a sub-wavelength scale

$$A(z) = e^{-\left(\frac{2\pi n_m}{\lambda}\left[\sin^2\theta - \left(\frac{n_d}{n_m}\right)^2\right]^{\frac{1}{2}} + \alpha\right)z}$$

n_m = refractive index of the metal,
n_d = refractive index of the dielectric,
θ = angle of illumination at the metal surface and
z = any location at which the evanescent field is measured.

$$\omega_p = \sqrt{\frac{4\pi n_e e^2}{m_e}}$$

$\omega_p = plasmon\ frequency$
n_e = Free electron density
$m_e = mass$
e = electron charge

Penetration depth(d_p) of the evanescent field is defined as given below.

$$d_p = \frac{\lambda}{2\pi\sqrt{n_m \sin^2\theta - n_d^2}}$$

The decay of evanescent field continues with distance.

R.G. Heideman, "Optical waveguide based evanescent field immunosensors", PhD Thesis, University of Twente, Enschede, 1993.

Patents

Patents:

- **Ram P. Gandhiraman,** Vivek Jayan, M. Meyyappan, Jessica Koehne. Atmospheric pressure plasma based fabrication of printable electronics and functional Coatings. US Patent application 14/515,072
- **Ram P. Gandhiraman,** Lourdes Basabe-Desmonts, Asif Riaz, Luke P. Lee, Ivan K. Dimov, Jens Ducree, Stephen Michael Daniels. "Method of surface treating microfluidic devices". PCT/EP2010/58631, US patent application 13/379,324, European patent application EP2442908, UK Patent application GB2471271
- **Ram P. Gandhiraman**, Vladimir Gubala, Cedric Volcke, Lourdes Basabe-Desmonts, Stephen Daniels. "A method for biomolecule immobilisation and minimisation of non-specific binding on surfaces for biomedical diagnostics". European Patent application No. EP09394010.4
- V. Gubala, **R.P. Gandhiraman**, N.C.H. Le, C. O'Mahony, S.M. Daniels, D.E.Williams. "Biocompatible coatings for non specific binding". US Patent Application number 13/049,086

Invention Disclosure:

- Niall O Connor, **Ram P. Gandhiraman**, David Williams, Stephen Daniels. "Aerosol assisted atmospheric plasma based surface modification and patterning for biosensors"
- **Ram P. Gandhiraman**, Gowri Manickam, Michael Berndt, David Williams, Stephen Daniels. "Plasma polymerized films with encapsulated metal nanoparticles as a substrate for SPR detection".

Acknowledgements

- Dr. Dennis Nordlund – SLAC National Accelerator Lab
- Jessica Koehne – NASA ARC
- Meyya Meyyappan – NASA ARC